

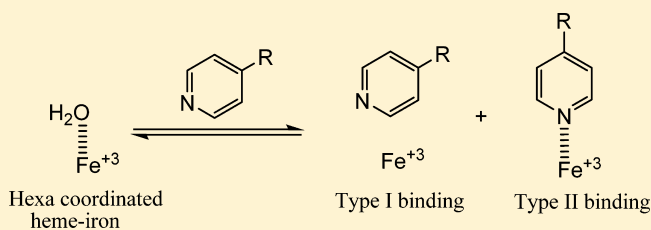
Comparative Study of the Affinity and Metabolism of Type I and Type II Binding Quinoline Carboxamide Analogues by Cytochrome P450 3A4

Upendra P. Dahal, Carolyn Joswig-Jones, and Jeffrey P. Jones*

Department of Chemistry, Washington State University, P.O. Box 644630, Pullman, Washington 99164-4630, United States

S Supporting Information

ABSTRACT: Compounds that coordinate to the heme-iron of cytochrome P450 (CYP) enzymes are assumed to increase metabolic stability. However, recently we observed that the type II binding quinoline carboxamide (QCA) compounds were metabolically less stable. To test if the higher intrinsic clearance of type II binding compounds relative to type I binding compounds is general for other metabolic transformations, we synthesized a library of QCA compounds that could undergo N-dealkylation, O-dealkylation, benzylic hydroxylation, and aromatic hydroxylation. The results demonstrated that type II binding QCA analogues were metabolically less stable (2- to 12-fold) at subsaturating concentration compared to type I binding counterparts for all the transformations. When the rates of different metabolic transformations between type I and type II binding compounds were compared, they were found to be in the order of N-demethylation > benzylic hydroxylation > O-demethylation > aromatic hydroxylation. Finally, for the QCA analogues with aza-heteroaromatic rings, we did not detect metabolism in aza-aromatic rings (pyridine, pyrazine, pyrimidine), indicating that electronegativity of the nitrogen can change regioselectivity in CYP metabolism.



INTRODUCTION

Cytochrome P450 (CYP) enzymes are a superfamily of heme thiolate proteins that can insert an atom of oxygen from molecular oxygen into many organic compounds. More than 80% of the clinically used drugs are metabolized by CYP enzymes.¹ In humans, 57 genes were identified that code for various CYP enzymes. Cytochrome P450 3A4 (CYP3A4) is the most abundantly expressed isoform in liver and comprises as much as 60% of total CYP enzymes.^{2,3} CYP3A4 contributes to the metabolism of more than 50% of marketed drugs,^{4,5} and it is often involved in unwanted drug–drug interactions. Because of the ubiquitous nature of CYP enzymes in body tissues and their ability to metabolize multiple organic compounds containing wide variety of functional groups,⁶ metabolic stabilization of drugs is a challenge in drug optimization process. Drugs need to be metabolized so that they can be excreted; however, drugs should be stable enough so that they can reach the site of the action. Hence, optimization of drug metabolism by CYP enzymes is always a goal during drug design and development.

CYP enzymes contain heme as a cofactor. The heme is tethered to the enzyme by a thiolate bond with cysteine. In resting state of the enzyme, iron of the heme is hexa-coordinated (coordinated with four nitrogen of porphyrin system, with the sulfur of cysteine proximally and with water distally) and is in low-spin state. According to the consensus mechanism for CYP,^{1,7} the catalytic cycle of CYP reaction begins with displacement of water by a substrate that converts hexa-coordinated low spin heme-iron(III) into pentacoordi-

nated high spin state (see Figure 1). Reduction of the iron(III) into iron(II) by cytochrome P450 reductase with the cofactor NADPH is followed by binding of a molecular oxygen into heme-iron(II). It has been hypothesized that formation of the high-spin pentacoordinated heme-iron(III) is required to initiate the catalytic cycle.^{1,8} Binding of a compound leading to an increase in formation of the high-spin penta-coordinated iron(III) is observable in the UV spectra and is called type I binding (Figure 2). If a substrate has a sterically unhindered aromatic nitrogen, the molecule can bind with heme-iron which will prevent formation of the high-spin pentacoordinated heme-iron. This binding mode, which leads to an increase in low-spin hexa-coordinated iron(III), is known as type II binding (Figure 2). The two binding modes, namely type I and type II, can be easily differentiated spectrophotometrically and were discovered more than 4 decades ago.^{9–11}

Since type II binding compounds have a higher affinity for CYP enzymes compared to similar type I binding compounds, type II binding compounds are extensively used as inhibitors of CYP enzymes.^{12–14} It has been assumed that type II binding of a molecule would lead to a dead-end complex and that the drug cannot be metabolized or that metabolism would be slowed. This leads to the hypothesis that type II binding compounds are metabolically more stable than the type I binding compounds.^{15,16} Contrary to this hypothesis, Peng et al.¹⁷ revealed that CYP3A4 can metabolize a series of type II binding

Received: September 12, 2011

Published: November 16, 2011

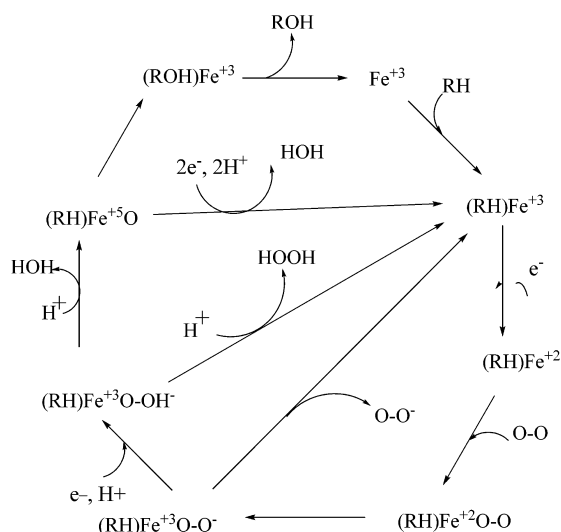


Figure 1. Consensus mechanism of cytochrome P450 enzymes. Fe^{3+} represents the pentacoordinated heme-iron in resting state of CYP enzymes.

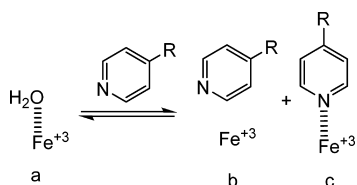


Figure 2. Binding modes of CYP enzymes. Fe^{3+} represents the pentacoordinated heme-iron: (a) low-spin heme-iron in wild type enzyme; (b) high-spin heme-iron in type I binding mode; (c) low-spin heme-iron in type II binding mode.

compounds significantly at subsaturating concentrations. More recently we¹⁸ reported that two type II binding quinoline carboxamide (QCA) compounds were metabolized more quickly than a similar type I binding QCA compound. We observed aromatic hydroxylation on the naphthalene ring of the QCA analogs. On the basis of the results from kinetics assay, electrochemical measurements, and surface plasmon resonance analysis, we proposed a direct reduction kinetic model for the metabolism of those type II binding compounds. Although it has been confirmed that the type II binding mode contributes to the observed high affinity,^{12,19–22} it is still a subject of debate whether type II binding increases the metabolic stability of these compounds. The answer can only be assessed by a systematic comparison of metabolic rates between type I and type II binding compounds.

CYP enzymes catalyze a number of transformations, for example, aliphatic hydroxylation, aromatic hydroxylation, N-dealkylation, O-dealkylation, epoxidation, S-oxidation, and N-oxidation. To compare affinity, metabolic stability, and

regioselectivity of various metabolic transformations between type I and type II binding compounds, we synthesized a library of QCA analogues. The library contained multiple series of type I and type II binding compounds with different functional groups on the same core structure. The binding mode of each compound was determined using UV/vis difference spectrum, and saturation kinetics was carried out to determine the kinetic parameters.

RESULTS

Design of the Substrates and Metabolite Quantification. In an attempt to systematically compare affinity and kinetic parameters of type I and type II binding compounds, a QCA core was derivatized to get a library of compounds (Figure 3). To probe the different types of oxidation carried out by the CYP enzymes, four different functional groups were coupled in the amide position of the QCA, namely, benzene, toluene, anisole, and *N,N*-dimethylaniline. Similarly the 2-position of the quinoline ring of QCA was incorporated with benzene, pyridine, pyrazine, or pyrimidine to change the binding mode as well as to investigate the role of various aza-heteroaromatic rings in binding mode and in metabolism. All of the substrate were synthesized by the method developed in our lab¹⁷ with a few modifications as shown in Scheme 1. Series 1 compounds are designed without aza-aromatic ring so that they can act as type I substrates. Series 2 compounds are designed with pyrid-4-yl at position 2 of the quinoline ring; these compounds are type II substrate because of the presence of accessible aromatic nitrogen. Series 3 compounds are designed with pyrid-2-yl at position 2 of the quinoline ring. These compounds are type I substrates, as they do not have accessible aromatic nitrogen but are electronically equivalent to series 2 type II substrates. Series 4 and series 5 compounds are designed to compare the effect of multiple nitrogens in a single aromatic ring, and they contain pyrazine and pyrimidine in position 2 of the quinoline ring, respectively.

To quantify the metabolites formed enzymatically, at least one metabolite per substrate was synthesized. The standard curve was prepared using an internal standard (phenacetin) versus the standard synthesized metabolite. Although multiple metabolites were observed for most of these compounds, ionization potentials of all of the metabolites from a substrate were assumed to be same with the synthesized metabolite for the purpose of quantification. Hence, the same standard curve was used for all the metabolites of a substrate. Structures of the substrates and the synthesized metabolites are presented in Table 1.

Binding Spectra. The type I binding mode has a difference spectrum with a Soret maximum at 385–390 nm and a trough at around 420 nm, whereas type II binding mode has a difference spectrum with a Soret maximum at 420–435 nm and a trough at 390–405 nm.^{10,11} The binding mode of the substrates was determined in purified enzyme using a split

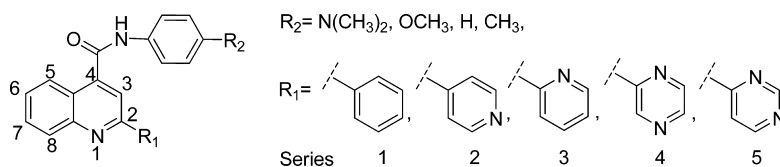


Figure 3. Quinoline carboxamide (QCA) core derivatization to build the library of compounds with different functional groups at the amide position and different aromatic rings at position 2.

Scheme 1. Synthesis of Quinoline Carboxamide Model Compounds

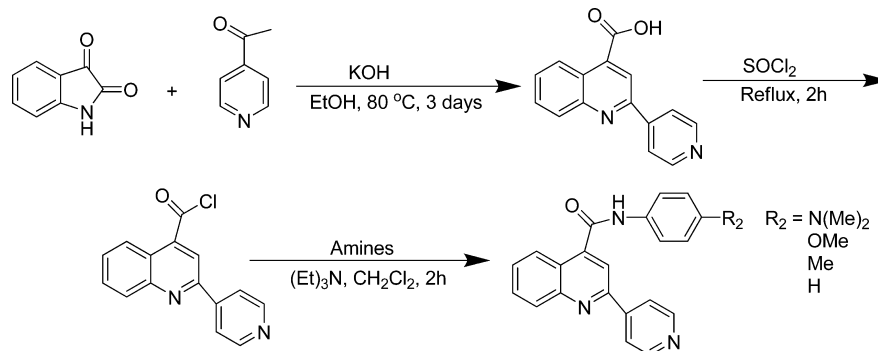
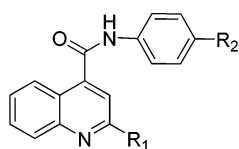


Table 1. Structures of the Substrates Used for the Study and Structures of the Metabolites Synthesized To Quantify the Metabolites Formed during the Enzymatic Assay^b



Series	R ₁	Substrate R ₂	Substrate ^a	Metabolite R ₂	Metabolite ^a
1		OCH ₃	1	OH	1M
		N(CH ₃) ₂	2	NH(CH ₃)	2M
		H	3	OH	1M
		CH ₃	4	CH ₂ OH	4M
2		OCH ₃	5	OH	5M
		N(CH ₃) ₂	6	NH(CH ₃)	6M
		H	7	OH	5M
		CH ₃	8	CH ₂ OH	8M
3		OCH ₃	9	OH	9M
		N(CH ₃) ₂	10	NH(CH ₃)	10M
		H	11	OH	9M
		CH ₃	12	CH ₂ OH	12M
4		OCH ₃	13	OH	13M
		N(CH ₃) ₂	14	NH(CH ₃)	14M
		H	15	OH	13M
		CH ₃	16	CH ₂ OH	16M
5		OCH ₃	17	OH	17M
		N(CH ₃) ₂	18	NH(CH ₃)	18M
		H	19	OH	17M
		CH ₃	20	CH ₂ OH	20M

^aSee Experimental Section for procedure of synthesis. ^bThe synthesized metabolite was a major metabolite formed during the bioassay for the corresponding substrate.

beam Olis spectrophotometer. Obtaining type II binding spectra is challenging,²³ and in addition the QCA analogues showed absorbance in the visible range, making determination of difference spectra particularly difficult. To overcome the problems, we used two chambered cuvettes, as shown in Figure 4, to determine the binding mode. Absorbance of the compounds along with binding mode is presented in Table 2. As expected, 2-phenyl QCA analogues and 2-pyridin-2-yl QCA analogues produced type I binding difference spectra whereas 2-pyridin-4-yl QCA, 2-pyrimidin-4-yl QCA, and 2-pyrazin-2-yl QCA analogues produced type II binding difference spectra. The difference spectra of a representative compound from each series are presented in Supporting Information (Figure S1).

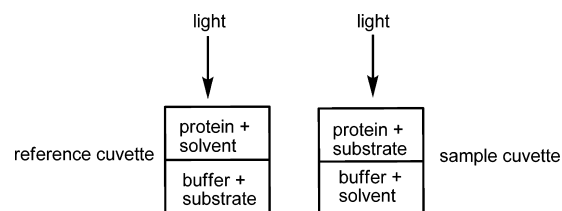


Figure 4. Schematic picture of two chambered cuvettes used to correct absorbance of substrate during binding mode determination.

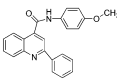
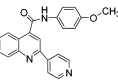
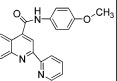
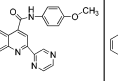
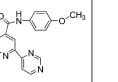
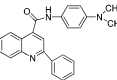
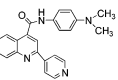
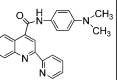
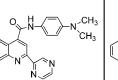
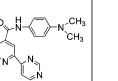
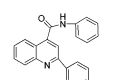
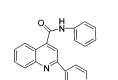
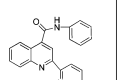
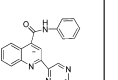
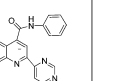
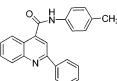
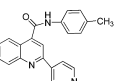
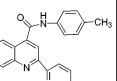
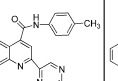
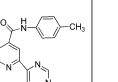
Table 2. UV–Visible Absorbance (Difference Spectra) To Determine Binding Mode of the Compounds^a

series	compd	Soret peak (nm)	Soret trough (nm)	binding mode ^b
1	1	388	415	type I
	2	385	416	type I
	3	392	417	type I
	4	393	417	type I
2	5	427	391	type II
	6	427	392	type II
	7	427	394	type II
	8	428	392	type II
3	9	388	417	type I
	10	386	416	type I
	11	389	418	type I
	12	391	416	type I
4	13	423	396	type II
	14	425	393	type II
	15	427	397	type II
	16	422	391	type II
5	17	425	391	type II
	18	422	392	type II
	19	424	390	type II
	20	425	390	type II

^aA representative spectrum of each series is presented in Supporting Information. ^bType I binding mode has a difference spectrum with a maximum at 385–390 nm and a trough at 415–420 nm. Type II binding mode has a difference spectrum with a maximum at 420–435 nm and a trough at 390–405 nm.

Affinity Differences between Type I and Type II QCA Analogues. Affinities of the QCA compounds with CYP3A4 were measured in terms of inhibition constants (K_i). Testosterone was used as a substrate to determine the inhibition constants. The results of inhibition assays are presented in Table 3. The K_i values are an average of triplicate assays. It was observed that the affinity of the type II binding compounds is higher than the affinity of their type I binding

Table 3. Inhibition Constants (K_i), Turnover Number (k_{cat}), Michaelis–Menten Constants (K_M), and in Vitro Intrinsic Clearance (V/K) of the Quinoline Carboxamide Analogues^a

Series	1	2	3	4	5
Structure					
K_i (μM)	3.1 ± 0.9	0.54 ± 0.1	11.9 ± 3.1	20.1 ± 3.0	2.2 ± 0.4
k_{cat} (min^{-1})	4.9 ± 0.5	3.1 ± 0.7	5.7 ± 0.5	5.36 ± 0.03	8.7 ± 0.1
K_M (μM)	2.2 ± 0.4	0.7 ± 0.3	2.6 ± 0.4	1.6 ± 0.1	2.6 ± 0.4
V/K ($\mu\text{M}^{-1} \text{min}^{-1}$)	2.2	4.4	2.2	3.4	3.3
Structure					
K_i (μM)	14.4 ± 1.7	0.80 ± 0.06	32.9 ± 0.9	15.93 ± 1.4	8.4 ± 0.6
k_{cat} (min^{-1})	27.9 ± 0.8	13.1 ± 0.5	10.5 ± 0.3	30.8 ± 2.0	9.6 ± 0.2
K_M (μM)	2.9 ± 0.3	1.03 ± 0.09	10.5 ± 0.5	11.1 ± 0.9	2.8 ± 0.1
V/K ($\mu\text{M}^{-1} \text{min}^{-1}$)	9.6	12.7	1.0	2.8	3.4
Structure					
K_i (μM)	4.1 ± 0.3	0.7 ± 0.1	14.5 ± 2.7	6.9 ± 0.3	2.2 ± 0.4
k_{cat} (min^{-1})	8.3 ± 0.6	13.7 ± 0.3	9.5 ± 0.2	8.9 ± 0.3	10.6 ± 0.3
K_M (μM)	6.5 ± 1.6	1.13 ± 0.06	7.1 ± 0.3	3.6 ± 0.1	3.3 ± 0.2
V/K ($\mu\text{M}^{-1} \text{min}^{-1}$)	1.3	12.1	1.3	2.5	3.2
Structure					
K_i (μM)	3.97 ± 0.06	0.54 ± 0.07	3.9 ± 0.1	2.7 ± 0.6	3.0 ± 1.0
k_{cat} (min^{-1})	41.0 ± 1.8	7.39 ± 0.07	37.4 ± 3.2	26.0 ± 1.1	12.8 ± 0.4
K_M (μM)	12.0 ± 1.4	0.76 ± 0.06	13.0 ± 1.8	8.0 ± 0.5	3.2 ± 0.4
V/K ($\mu\text{M}^{-1} \text{min}^{-1}$)	3.4	9.7	2.9	3.3	4.0

^aKinetic parameter values represent the mean of triplicate assays, and values after “±” represent standard deviation.

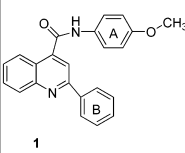
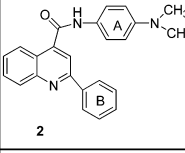
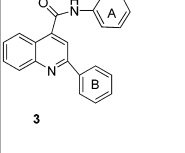
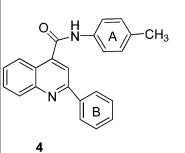
counterparts (specifically 7- to 21-fold higher affinity for type II binding compounds in series 2 compared to type I binding compounds in series 3). 2-Pyridin-2-yl QCA analogues (series 2, type II binders) showed strong affinity for CYP3A4, and all of the compounds of series 2 have K_i values in the nanomolar range. Type I binding compounds (series 1 and series 3) have K_i values in the range 3–33 μM . Type I binding compounds without nitrogen (series 1) have up to 4-fold lower K_i values compared to type I binding compounds with sterically hindered nitrogen (series 3) except compounds with tolyl group (compound 4 vs compound 12), whose K_i values are close to each other. Similarly, insertion of the second nitrogen in the pyridine ring of the type II binding compounds increased the K_i values from 3- to 37-fold (series 2 to series 4 and 5).

Saturation Kinetics. To determine the kinetic parameters, we carried out a saturation kinetic assay. Five concentrations of substrate ranging from $0.2K_M$ to $5K_M$ were used to determine the Michaelis–Menten constant (K_M) and turnover number (k_{cat}). The kinetic parameters K_M , k_{cat} , and in vitro metabolic intrinsic clearance (V/K) are presented in Table 3. The k_{cat} values of type I binding compounds (series 1 and 3) are larger than type II binding compounds in series 2 except compounds

6 and 7. The K_{cat} value of type II binding compound 6 is more than 2-fold smaller than type I binding compound 2 of series 1, but k_{cat} value of compound 6 is 1.2 times larger than type I binding compound 10 of series 3. Type II binding compound 7 has about 1.5 times higher k_{cat} value than the type I binding compounds 3 and 11. This indicates that the rate of metabolism of type II binder is slower (with few exceptions) than the type I binding counterpart when the enzyme is saturated with substrate. Insertion of a second nitrogen in the pyridine ring generally increased the turnover number of type II binding compounds (series 2 to series 4 and series 5) with few exceptions.

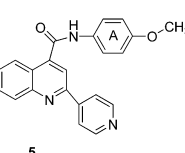
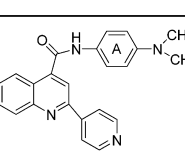
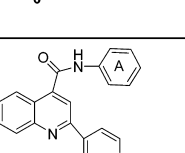
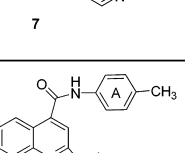
In vitro intrinsic clearance (V/K) is used in drug industry as an important predictor for the metabolic stability of a drug in vivo. V/K is a measure of the rate of clearance of a drug in subsaturating concentration of the substrate. V/K values of the type II binding compounds in series 2 were found to be 2- to 12-fold higher than electronically similar type I binding compounds in series 3. The V/K values of the type I binding compounds in series 1 were 1.3- to 4.7-fold lower than the type II binding compounds in series 2. Overall, the type II binding QCAs were metabolically less stable than the type I binding

Table 4. Comparison of O-Demethylation, N-Demethylation, Aromatic Hydroxylation, and Benzylic Hydroxylation in Type I Binding Quinoline Carboxamide Analogues^d

Structure	Metabolite	k_{cat} (min ⁻¹) ^a	K_M (μM) ^b	Ratio ^c
 1	O-Demethylation	4.2 ± 0.4	2.3 ± 0.4	5.8
	Aromatic hydroxylation at ring B	0.72 ± 0.05	2.0 ± 0.4	
	Total	4.9 ± 0.5	2.2 ± 0.4	
 2	N-Demethylation	27.9 ± 0.8	2.9 ± 0.3	∞
	Aromatic hydroxylation at ring B	0	0	
	Total	27.9 ± 0.8	2.9 ± 0.3	
 3	Aromatic hydroxylation at ring A	4.7 ± 0.3	5.3 ± 1.5	1.3
	Aromatic hydroxylation at ring B	3.7 ± 0.3	8.9 ± 1.5	
	Total	8.3 ± 0.6	6.5 ± 1.6	
 4	Benzylic hydroxylation	34.8 ± 1.1	11.3 ± 1.1	6.0
	Aromatic hydroxylation at ring B	5.8 ± 0.4	14.4 ± 2.8	
	Total	41.0 ± 1.8	12.0 ± 1.4	

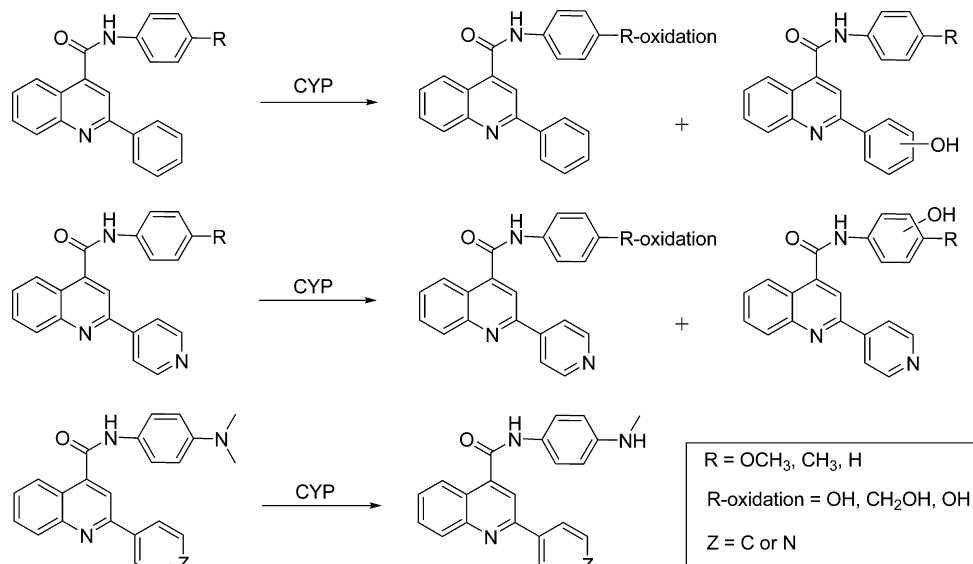
^aTurnover number. ^bMichalies–Menten constant. ^cRatio of product formation from functional group oxidation at ring A to aromatic hydroxylation at ring B. ^dKinetic parameter values represent the mean of triplicate assays, and values after “±” represent standard deviation.

Table 5. Comparison of O-Demethylation, N-Demethylation, Aromatic Hydroxylation, and Benzylic Hydroxylation in Type II Binding Quinoline Carboxamide Analogues^d

Structure	Metabolite	k_{cat} (min ⁻¹) ^a	K_M (μM) ^b	Ratio ^c
 5	O-Demethylation	1.8 ± 0.4	0.8 ± 0.3	1.4
	Aromatic hydroxylation at ring A	1.3 ± 0.2	0.70 ± 0.09	
	Total	3.1 ± 0.7	0.7 ± 0.3	
 6	N-Demethylation	13.1 ± 0.5	1.3 ± 0.5	∞
	Aromatic hydroxylation at ring A	0	0	
	Total	13.1 ± 0.5	1.3 ± 0.5	
 7	p-Hydroxylation at ring A	7.8 ± 0.2	1.07 ± 0.09	1.3
	Aromatic hydroxylation at ring A	5.9 ± 0.4	1.24 ± 0.05	
	Total	13.7 ± 0.4	1.13 ± 0.06	
 8	Benzylic hydroxylation	6.0 ± 0.1	0.77 ± 0.07	4.4
	Aromatic hydroxylation at ring A	1.37 ± 0.04	0.72 ± 0.06	
	Total	7.39 ± 0.07	0.76 ± 0.06	

^aTurnover number. ^bMichalies–Menten constant. ^cRatio of product formation from functional group oxidation at ring A to aromatic hydroxylation at ring A. ^dKinetic parameter values represent the mean of triplicate assays, and values after “±” represent standard deviation.

Scheme 2. Metabolic Transformations by CYP3A4



counterparts. Insertion of nitrogen in type I binding compounds (series 1 to series 3) as well as type II binding compounds (series 2 to series 4 and 5) decreased the intrinsic clearance (Table 4).

Comparison of O-Demethylation, N-Demethylation, Aromatic Hydroxylation, and Benzylic Hydroxylation between Type I and Type II Binding Compounds.

The kinetic parameters for O-demethylation, N-demethylation, aromatic hydroxylation, and benzylic hydroxylation for type I binding 2-phenyl QCA analogues (series 1) are presented in Table 4 and those of type II binding 2-pyridin-4-yl QCA analogues (series 2) are presented in Table 5. Functional group oxidation as well as hydroxylation of the benzene ring at position 2 of the 2-phenyl QCA (series 1) was observed except in compound 2 with *N,N*-dimethyl functional group (Scheme 2). Metabolism in the 2-aza-heteroaromatic rings (pyridine, pyrimidine, and pyrazine) of the QCA analogues (series 2, 3, 4, 5) was not detected within the detection limit of the instrument. The rates of functional group oxidation were compared in reference to the aromatic hydroxylation in ring B of the same compound (see Table 4 for the ratio of the rate of functional group oxidation to the rate of aromatic oxidation; the bigger ratio indicates faster rate of metabolism for the functional group) for type I binding compounds (series 1), and the regioselectivity of metabolism was found to be in the order of N-demethylation > O-demethylation ~ benzylic hydroxylation > aromatic hydroxylation. The order of rates of functional group transformation for the type II binding compounds (series 2) was determined in reference to the aromatic hydroxylation in the ring A (see Table 5 for the ratio of the rate of functional group oxidation to the rate of aromatic oxidation), and the order of regioselectivity of metabolism was found to be N-demethylation > benzylic hydroxylation > O-demethylation ~ aromatic hydroxylation.

DISCUSSION

Aromatic nitrogen can coordinate with the heme-iron of CYP enzymes to maintain a low-spin state in type II binding mode. The reduction potential of the type II bound heme-iron is higher than the type I bound heme-iron.¹⁸ This higher

reduction potential was considered to be a major contributor to the metabolic stability^{12,15,16} of type II binding compounds compared to type I binding compounds, and hence type II binding compounds are assumed to be inhibitors of CYP enzymes. Inhibition of CYP enzymes can lead to a high risk of drug–drug interactions with potentially serious clinical implications.²⁴ Therefore, it is an important goal in drug industry to get optimum metabolic stability and inhibitory potential of the drug candidate during the drug development and design. Recently we reported that the affinity of a compound can be increased by more than 4200-fold just by changing the position of nitrogen in QCA.²¹ Our earlier study involving electrochemistry, surface plasmon resonance, and saturation kinetics revealed the kinetic pathway for the metabolism of type II binding QCA compounds via direct reduction of heme-iron in type II binding mode.¹⁸ In the past study we used QCA analogues with naphthalene moiety and observed aromatic hydroxylated metabolites. In this study we synthesized five series of compounds with four different functional groups so that we can compare the four transformations, namely, N-demethylation, O-demethylation, benzylic hydroxylation, and aromatic hydroxylation. We coupled the different binding motifs, namely, phenyl, pyridinyl, pyrazinyl, pyrimidyl at the 2 position of quinoline to compare the metabolic stability and regioselectivity of type II binding QCA compounds to that of structurally similar type I binding QCA compounds.

The library of compounds we chose to use in the *in vitro* assay allows for the systematic comparison of kinetic parameters between type I and type II binding compounds and was based on the hypothesis that the sterically accessible aromatic nitrogen is required for type II binding compounds.²¹ To accomplish this goal, we synthesized the QCA analogues with 2-pyridin-4-yl (series 2), which can type II bind with CYP3A4 (Figure 3). For a type I binding counterpart, we synthesized 2-phenyl QCA analogues (series 1) and 2-pyridin-2-yl QCA analogues (series 3). The series 3 compounds are electronically similar to the type II binding series 2 compounds; however, series 1 compounds are deprived of nitrogen in the aromatic ring at position 2 of QCA. To investigate the effect of insertion of a second nitrogen in pyridine ring, 2-pyrimidin-4-yl

QCA analogues (series 4) and 2-pyrazin-2-yl QCA analogues (series 5) were synthesized. As expected, ligands in series 1 and series 3 produced type I binding difference spectra because of the absence of accessible nitrogen to coordinate with the heme-iron. The sterically hindered ortho-nitrogen of pyridine in series 3 analogues could not coordinate with heme-iron²¹ and produced type I binding difference spectrum. Both meta- and para-nitrogen of aza-heteroaromatic rings at position 2 of the QCA analogues (series 2, 4, and 5) coordinated with heme-iron to give the type II binding difference spectra.

The affinity of the type II ligands is higher because of the coordination of the electron rich nitrogen with the electron deficient heme-iron.¹⁷ Replacing the 2-phenyl ring of the QCA analogues with the 2-pyridin-4-yl ring increased the affinity from 6- to 18-fold (series 1 to series 2), indicating that the type II ligands contributed to the higher affinity with the heme-iron. The 2-pyridin-2-yl QCA analogues (series 3) cannot coordinate with the heme-iron because of steric hindrance but has the same electronic core as type II ligands of series 2. The series 3 compounds have lower affinity (7- to 41-fold) with CYP3A4 compared to series 2 compounds, demonstrating that direct coordination to heme-iron by an aromatic nitrogen is contributing to the higher affinity. QCA analogues with sterically hindered nitrogen in an aromatic ring (series 3), which cannot bind in type II binding mode, have lower affinity than the QCA analogues without nitrogen in the aromatic ring (series 1). Both series 1 and series 3 compounds are type I binding compounds, but series 3 has a nitrogen in an aromatic ring which did not contribute to type II binding. Series 3 compounds had about 4-fold lower affinity than series 1 compounds except compound 4 and compound 12, which showed about same affinity. Affinity of type II binding compounds with two nitrogens in an aromatic ring is lower than that of the type II binding compounds with one nitrogen in aromatic ring. Affinity of the type II ligands containing two nitrogens in a ring (2-pyrazin-2-yl and 2-pyrimidin-4-yl) of series 4 and series 5 was lower than that of series 2 which has only one nitrogen, possibly because of (a) a decrease in the electron density of the coordinating nitrogen²⁵ by electronegativity effect of the inserted second nitrogen and/or (b) an unfavorable interaction of the second nitrogen with amino acids in the active site of the enzyme and/or (c) an increased water solubility of the substrates on inserting a nitrogen which can change the partition equilibrium between polar aqueous phase and lipophilic active site. These possibilities are under investigation in our lab.

It has been speculated that the higher reduction potential of the type II ligand–enzyme complex is a reason¹⁶ for higher inhibitory potential of the type II binding compounds. However, the electrochemical measurement of the reduction potential in type I and type II ligands showed only a 2-fold difference¹⁸ in the rate of reduction, indicating the possibility for the metabolism of the type II ligands. We observed that the k_{cat} of the type II binding compounds in series 2 is generally lower or comparable to the k_{cat} of the type I binding compounds in series 1 and series 3, in agreement with the lower reduction rate for the type II ligand–enzyme complex compared to the type I ligand–enzyme complex. In series 2 (which are all type II binding compounds) 5 has a lower k_{cat} than compounds 1 and 9, 8 has a lower k_{cat} than compounds 4 and 12, while 6 has a lower k_{cat} than compounds 2 but not compound 10, and compound 7 has about the same k_{cat} as compounds 3 and 11. While the agreement between binding

mode and k_{cat} is not perfect, it most likely reflects a slower rate of reduction combined with differences in binding orientation. For all the compounds in series 2 the reported off rate for type II binding QCA analogue¹⁸ (0.006–0.03 s⁻¹) is slower than the k_{cat} of type II binding compounds 0.05–0.5 s⁻¹ (Table 3). Since k_{cat} the overall rate of the metabolism for all the steps in the catalytic cycle, is faster than the debinding rate of type II binding compounds, it is unlikely that the substrate debinds before reduction. Hence, the type II binding QCA compounds are expected to follow the direct reduction pathway as described by Pearson et al.¹⁸

The in vitro intrinsic metabolic clearance (V/K) is the determinant of the metabolic stability of the compounds in subsaturating concentration of the enzyme. It is worth noting that clinical drugs are normally administered at subsaturating concentration of substrate. The V/K values for the series 2 compounds are up to 3-fold higher than the series 1 compounds and up to 12-fold higher than the series 3 compounds, indicating that type II binding compounds get metabolized more quickly in subsaturating concentration of the substrate, in agreement with previously reported results.¹⁸ The intrinsic clearance of the type II binding compounds with multiple nitrogens in an aromatic ring is lower than the single nitrogen containing counterpart, indicating that tightly bound type II ligands get metabolized more quickly than the loosely bound type II ligands. In spite of higher reduction potential and lower k_{cat} the type II binding QCA analogues get metabolized more quickly in subsaturating concentration because of their higher affinity for the enzyme.

We did not detect aza-aromatic ring hydroxylation for any of the four series of heteroaromatic rings at position 2 of QCA analogues (Figure 3) within our instrument's detection limit. Electronegative nitrogen in an aza-aromatic ring can reduce electron density of carbons of the aromatic ring. The oxy-iron species of the CYP enzyme is electrophilic in nature; hence, the decrease in electron density in the aromatic ring is likely the reason for the metabolic stability of the aza-aromatic ring. Thus, incorporation of nitrogen in the aromatic ring results in branching to alternative sites of metabolism.

To investigate if regioselectivity is altered between type I and type II ligands for different types of metabolic transformations, we compared QCA analogues that could undergo O-demethylation, N-demethylation, aromatic hydroxylation, and benzylic hydroxylation. The comparison of the different transformations was based on the ratio of the functional group transformation of interest to aromatic hydroxylation in the same compound. In type I binding compounds of series 1, we observed aromatic hydroxylation in the 2-phenyl ring of QCA; hence, for the comparison the ratio of functional group transformation to that of the 2-phenyl ring hydroxylation (Table 4) was considered. In type II binding series 2 compounds, the pyridine ring was not metabolized but we observed metabolism in the benzene ring A (Table 5) which also contains a functional group of interest for the transformation; hence, the regioselectivity was determined with reference to the aromatic hydroxylation in ring A. For the compounds undergoing N-demethylation, we did not observe aromatic hydroxylation (Scheme 2), indicating N-demethylation outcompetes the aromatic hydroxylation in both type I and type II ligands. In the case of type I binding compounds (series 1), O-demethylation and benzylic hydroxylation have about same relative rate of metabolism and the aromatic hydroxylation is the slowest of the transformations under the

investigation. Rates obtained for each transformation were similar to that of the reported activation energy for the transformations using *in silico* methods.^{26–29} In the case of type II binding compounds, the trend of transformation is same as that of the type I binding compounds except that the benzylic hydroxylation in compound **8** is about 3-fold faster compared to O-demethylation of compound **5**. In all the transformations, the K_M values stay the same within experimental error for the two metabolites observed, indicating the common binding site³⁰ for both transformations by the CYP3A4.

Thus, for this series of compounds, metabolic stability is not increased by nitrogen substitution in a single aromatic ring, since this substitution results in branching to a different metabolite. To decrease metabolism and still have a strong inhibitor, a second alteration would be required at the site of the branched metabolism. For example, benzylic and aromatic hydroxylation could be stopped by introducing fluorine at the site of metabolism. Another alternative or complementary strategy would be to introduce a nitrogen atom in into the “A ring” (see Table 4), which would slow aromatic hydroxylation on that ring. If a decrease in inhibitory potency is desired with increased metabolic stability, then nitrogen substitution ortho to the quinoline linkage seems to work best. Such a substitution has the electronic effect of slowing metabolism, but since it does not coordinate to the iron, these compounds have much lower inhibitory potency.

In conclusion, a comparative study between type I and type II binding compounds using a library of QCA analogues was undertaken with compounds having the same structural core but differing in number and position of nitrogen. The type II binding compounds showed higher affinity than the type I binding counterparts. We observed that the turnover numbers (k_{cat}) of the type II binding compounds were lower than the type I binding compounds. More importantly we observed that the *in vitro* intrinsic metabolic clearance, as measured by V/K , for type II binding compounds was up to 12-fold higher than the structurally similar type I binding counterparts. The insertion of a second nitrogen in heteroaromatic ring of the type II ligands decreased the affinity and the intrinsic clearance. The order of the metabolic rates for four studied metabolic transformations by CYP3A4 was found to be N-demethylation > benzylic hydroxylation > O-demethylation > aromatic hydroxylation in type both I and type II binding compounds.

■ EXPERIMENTAL SECTION

Materials and Instruments. Solvents and chemicals were purchased from Aldrich (St. Louis, MO), Fisher Scientific (Pittsburgh, PA), EMD (Gibbstown, NJ), and Mallinckrodt Baker (Phillipsburg, NJ) and used without purification. CYP3A4 baculosomes were a generous gift from Tom Rushmore. ¹H NMR spectra were obtained using a 300 MHz spectrometer equipped with a quad-detection probe (¹H, ¹³C, ³¹P, and ¹⁹F). ¹H-decoupled ¹³C NMR results were obtained at 75 MHz. Mass spectrometry was performed on a ThermoQuest Surveyor coupled to Thermo-Finnigan LCQ Advantage ESI-MS. Absorbance spectra were collected on a double-beam Olis upgraded Aminco DW-2000 spectrometer.

Enzyme Expression and Purification. The CYP3A4 NF14 construct was purified and expressed from *Escherichia coli* as described by Roberts.³¹ The purity was >95% as determined by SDS–PAGE analysis. The CYP3A4 concentration was determined by absorbance at 450 nm using an extinction coefficient of 91 mM⁻¹ cm⁻¹³² for the carbon monoxide bound protein. The purified CYP3A4 was stored in 100 mM potassium phosphate (pH 7.4) buffer with 20% glycerol at –80 °C.

Binding Spectra. Difference binding spectra were collected on a double-beam Olis upgraded Aminco DW-2000 spectrometer (Olis Inc., Bogart, GA). A baseline was recorded with protein in both reference and sample cuvettes before collecting the difference spectra. To correct the absorbance from the QCA substrates, two chambered cuvettes (NSG Precision Cells Inc., Farmingdale, NY) were used. Purified CYP3A4 (0.5 μM) was added to the sample and reference cuvettes, and an equal volume of 100 mM potassium phosphate buffer, pH 7.4, was added in the other chamber of the both cuvettes. Substrate (20 μM final concentration) was added in the protein chamber of the sample cuvette and the buffer chamber of the reference cuvette. To correct for dilution, an equal volume of solvent used to add the substrate was also added in the protein chamber of the reference cuvette and the buffer chamber of the sample cuvette. Absorbance was recorded from 350 to 500 nm to determine the mode of binding.

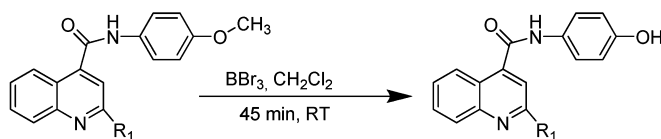
Inhibition Study. Testosterone was used as a CYP3A4 substrate, and K_i values were determined from the formation rate of 6-β-hydroxytestosterone. Four different final concentrations (30, 60, 90, and 120 μM) of testosterone in 100 mM potassium phosphate buffer at pH 7.4 were used. Three different inhibitor concentrations were added to each different concentration of testosterone, and one set was incubated without inhibitor. CYP3A4 baculosomes (4 pmol) were added to the incubation mixtures containing substrate and inhibitor. After preincubation of the mixture for 5 min at 37 °C, NADPH was added to a final concentration of 1 mM to initiate the reaction. The final volume of all the incubations was 0.5 mL. At the end of the 10 min incubation the reactions were quenched by adding 200 μL of acetonitrile containing internal standard phenacetin (25 μM). The enzyme was removed by centrifugation (Eppendorf centrifuge 5415D) for 10 min at 16000g, and the formation of product was analyzed by HPLC with UV detection. The HPLC system used reverse phase chromatography (Alltech, Altima C18 5 μm, 150 mm length, 3.2 mm i.d.), beginning with 95% mobile phase A (0.1% trifluoroacetic acid in water) and 5% mobile phase B (0.1% trifluoroacetic acid in acetonitrile) with linear gradient to 65% mobile phase B over 25 min. All the compounds were found to be competitive inhibitors based on graphical analysis using reciprocal plots. Each compound's K_i was determined based on the best fit to the Michaelis–Menten equation for competitive inhibition using GraphPad Prism 4 (San Diego, CA) graphing software.

Saturation Kinetics. At least five final concentrations (0.2 K_M to 5 K_M) of substrates were used to determine the kinetic parameters for the metabolism by CYP3A4. CYP3A4 baculosomes (4 pmol) were added to the incubation mixtures containing a substrate in 100 mM potassium phosphate buffer at pH 7.4 followed by preincubation for 5 min at 37 °C. NADPH was added to a final concentration of 1 mM to initiate the reaction. The final volume of all incubations was 0.5 mL. Reactions were quenched after 10 min by adding 200 μL of acetonitrile containing phenacetin (25 μM) as an internal standard. The enzyme was removed by centrifugation (Eppendorf centrifuge 5415D) for 10 min at 16000g, and metabolites were analyzed by LC/MS (Thermo Quest HPLC series coupled with Thermo Finnigan LCQ Advantage). The HPLC system used reverse phase chromatography (Agilent, Eclipse plus C18 5 μm, 150 mm length, 3.2 mm i.d.) beginning with 85% of mobile phase A (0.1% acetic acid in water) and 15% mobile phase B (0.1% acetic acid in acetonitrile) with a linear gradient to 85% of mobile phase B over 25 min. The m/z was monitored for the internal standard and metabolites of the substrates. The kinetic constants were determined based on the best fit to the Michaelis–Menten equation using GraphPad Prism 4 (San Diego, CA) graphing software.

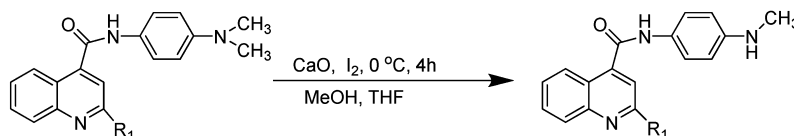
Metabolite Identification and Quantification. To identify the position of metabolism, LC/MS/MS analysis was carried out using a Thermo Quest HPLC coupled with Thermo Finnigan LCQ Advantage. The HPLC system used reverse phase chromatography (Agilent, Eclipse plus C18 5 μm, 150 mm length, 3.2 mm i.d.) beginning with 85% of mobile phase A (0.1% acetic acid in water) and 15% mobile phase B (0.1% acetic acid in acetonitrile) with a linear gradient to 85% of mobile phase B over 25 min. The fragments were monitored in a range of 100–450 m/z for the metabolites using the

Scheme 3. Synthesis of the Metabolites

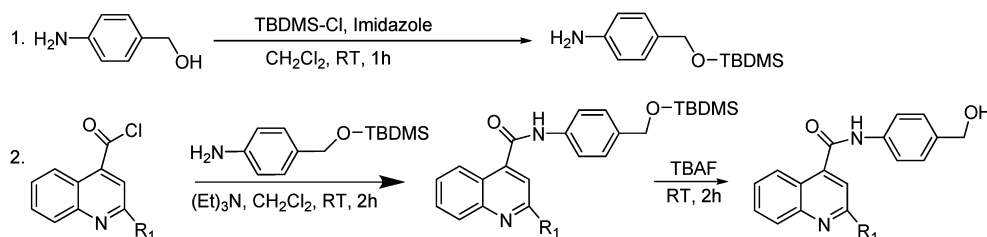
a) synthesis of aromatic hydroxylation metabolites



b) synthesis of N-demethylation metabolites



c) synthesis of benzylic hydroxylation metabolites



electrospray ionization (ESI) mode with collision energy of 40 V. The synthesized standard metabolites have the same retention time and fragmentation pattern as one of the metabolites obtained by CYP3A4 metabolism. The standard curve of the standard synthesized metabolite with the internal standard was used to quantify the metabolites formed.

Synthesis of Substrates. Substrates and metabolites were synthesized as described by Peng et al.²¹ with modifications as needed. The general synthetic methodology is described below in terms of synthesis of compound **1**. Synthesis of the other substrates and characterization data are presented in Supporting Information. Purity of the substrates was determined by reversed phase HPLC system. The HPLC was recorded on an Agilent 1100 series instrument equipped with an Alltech Altima C18 column (5 μ m, 150 mm length, 3.2 mm i.d.) and a UV detector. The solvent system starts with 95% mobile phase A (0.1% trifluoroacetic acid in water) and 5% mobile phase B (0.1% trifluoroacetic acid in acetonitrile) with linear gradient to 65% mobile phase B over 25 min. An indicated purity of >99% indicates that no other peaks in the chromatogram occur. All substrates reported in this publication were determined to have purities of >95%.

N-(4-Methoxyphenyl)-2-phenylquinoline-4-carboxamide (1). To a 100 mL round-bottom flask equipped with a water condenser and a stir bar were combined potassium hydroxide (842 mg, 15 mmol) and ethanol (5 mL). The reaction mixture was stirred at 80 °C to dissolve the potassium hydroxide. Isatin (736 mg, 5 mmol) was added to the reaction mixture followed by dropwise addition of acetophenone (661 mg, 5.5 mmol). The mixture was refluxed at 80 °C for 2 days. Then the solvent was evaporated using a rotary evaporator and the residue was dissolved in 50 mL of water. The aqueous phase was neutralized with dropwise addition of 1 N HCl to pH 6. The resulting solid was collected by vacuum filtration to get crude 2-phenylquinoline-4-carboxylic acid. The crude 2-phenylquinoline-4-carboxylic acid was used directly to synthesize acyl chloride. To the 50 mL round-bottom flask equipped with a water condenser and a stir bar were mixed the crude acid obtained above and 5 mL of neat thionyl chloride, and the mixture was refluxed at 80 °C. After 2 h excess thionyl chloride was evaporated using a stream of argon to get 2-phenylquinoline-4-carbonyl chloride. The resulting solid was dissolved

in 5:1 mixture of dichloromethane/triethylamine (10 mL) in a 50 mL round-bottom flask, and *p*-anisidine (677 mg, 5.5 mmol) was added. The reaction mixture was stirred at room temperature. After 2 h the solvent was evaporated using a rotary evaporator and the crude product was purified using flash chromatography (30 g silica gel 60, 0.063–0.200 mm) with 10% ethyl acetate in dichloromethane. The product obtained was crystallized in dichloromethane/ethanol to get pure *N*-(4-methoxyphenyl)-2-phenylquinoline-4-carboxamide in 38.8% overall isolated yield. ¹H NMR (CDCl₃) δ 3.85 (s, 3H), 6.96 (dt, J = 9.2, 2.2 Hz, 2H), 7.45–7.5 (m, 4H), 7.64–7.75 (m, 3H), 7.82 (s, 1H), 8.03–8.15 (m, 5H); ¹³C NMR (CDCl₃) δ 55.79, 114.61, 116.54, 122.18, 123.34, 125.17, 127.62, 127.69, 129.18, 130.05, 130.12, 130.59, 130.94, 138.65, 143.09, 148.78, 156.90, 157.21, 165.63; ESI-MS [$M + H$]⁺ = 355.4. Purity, \geq 99%.

Synthesis of Metabolites. Metabolites were synthesized as shown in Scheme 3.

O-Demethylation of the Substrate. The O-demethylation of the substrate was carried out as described elsewhere³³ with modification as needed (Scheme 3a). The general synthetic methodology for O-demethylation is described below in terms of synthesis of **1M**. Synthesis of the other metabolites and characterization data are presented in Supporting Information.

N-(4-Hydroxyphenyl)-2-phenylquinoline-4-carboxamide (1M). To the 10 mL solution of **1** (127 mg, 0.36 mmol) in CH₂Cl₂, boron tribromide (1 M in CH₂Cl₂, 1.1 mL, 1.1 mmol) was added over 2 min with stirring. The reaction mixture was stirred for 45 min at room temperature. The reaction was quenched by saturated sodium hydrogen carbonate, and the mixture was adjusted to pH 8 and was extracted with CH₂Cl₂ (3 \times 30 mL). The combined organic phase was washed with water. The solvent was removed under reduced pressure, and the residue was flash chromatographed using 10% EtOAc/CH₂Cl₂ followed by 30% MeOH/CH₂Cl₂. The isolated overall yield was 83%. ¹H NMR (DMSO) δ 6.77 (dt, J = 8.8, 2.2 Hz, 2H), 7.52–7.68 (m, 6H), 7.83 (ddd, J = 7.7, 7.0, 1.3 Hz, 1H), 8.13 (m, 1H), 8.29–8.37 (m, 3H), 9.35 (s, 1H), 10.57 (s, 1H); ¹³C NMR (DMSO) δ 115.85, 117.44, 122.41, 124.02, 125.90, 128.03, 129.62, 130.29, 130.63, 130.96, 131.19, 138.87, 144.00, 148.60, 154.70, 156.50, 165.35; ESI-MS [$M + H$]⁺ = 341.4.

N-Demethylation. A few methods were reported in literature for N-demethylation. We attempted N-demethylation using *N*-iodosuccinamide³⁴ and a selective N-demethylation method using a column chromatography-like setup by Rosenau et al.,³⁵ but they did not work in our hands. The N-demethylation method developed by Acosta et al.³⁶ using calcium oxide and iodine in the presence of methanol worked for all five series of our compounds (Scheme 3b).

The general synthetic methodology for N-demethylation is described below in terms of synthesis of **2M**. Syntheses of the other metabolites and characterization data are presented in Supporting Information.

***N*-(4-(tert-butylidimethylsilyloxy)phenyl)-2-phenylquinoline-4-carboxamide (2M).** To an ice chilled mixture of **2** (50 mg, 0.14 mmol) and CaO (61 mg, 1.1 mmol) in tetrahydrofuran (1.6 mL) and methanol (1.2 mL) was added iodine (69 mg, 0.27 mmol). The mixture was stirred at 0 °C until the reaction was completed. The reaction was monitored by TLC, and in 4 h all the reactant was consumed. The reaction mixture was filtered, and the filtrate was sequentially washed with 15% sodium thiosulfate solution, water, and brine solution. The organic phase was dried over magnesium sulfate, and solvent was evaporated in a rotary evaporator. The product was separated by flash chromatography using 4% acetone in dichloromethane. The product (**2M**) was crystallized in CH₂Cl₂/hexanes system to get 25 mg of pure product with an isolated yield of 55%. ¹H NMR (DMSO) δ 2.67 (d, *J* = 5.0 Hz, 3H), 5.58 (q, *J* = 5.3 Hz, 1H), 6.54 (d, *J* = 8.9 Hz, 2H), 7.51–7.59 (m, 5H), 7.64 (t, *J* = 8.2 Hz, 1H), 7.83 (t, *J* = 8.2 Hz, 1H), 8.16 (t, *J* = 9.1 Hz, 2H), 8.27 (s, 1H), 8.35 (d, *J* = 6.5 Hz, 2H), 10.43 (s, 1H); ESI-MS [*M* + *H*]⁺ = 354.3.

Benzylic Hydroxylation. Attempts to carry out direct benzylic hydroxylation were not successful. We attempted to convert the benzyl group into benzyl halide using *N*-bromosuccinimide/benzoyl peroxide system as performed by Dauben and McCoy,³⁷ using iodine/hydrogen peroxide system as performed by Barluenga et al.³⁸ and using bromine/dimethyl sulfoxide system as performed by Ghaffarzadeh et al.³⁹ We also tried to convert the benzyl group into benzaldehyde using ferric chloride/*tert*-butyl hydroperoxide system as performed by Nakanishi and Bolm⁴⁰ and using 2-iodoxybenzoic acid as performed by Nicolaou et al.⁴¹ As all these attempts did not work in our hands, we synthesized the benzylic metabolite by protecting 4-aminobenzyl alcohol and reacting protected benzylic alcohol with appropriate acid chlorides to get the protected benzylic alcohols which on deprotection yielded the desired benzylic hydroxylated metabolites (Scheme 3c). The general synthetic methodology of benzylic hydroxylated metabolites is described below in terms of the synthesis of **4M**. Synthesis of the other metabolites and characterization data are presented in Supporting Information.

4-(tert-butylidimethylsilyloxy)methyl)aniline. To a solution of 4-aminobenzyl alcohol (1.5 g, 12.2 mmol) in dichloromethane (20 mL) were added *tert*-butylidimethylsilyl chloride (TBDMSCl, 1.8 g, 12.2 mol) and imidazole (0.91 g, 13.4 mmol). After being stirred for 1 h at room temperature, the reaction mixture was diluted with brine solution and then extracted with ethyl acetate. The organic phase was dried over sodium sulfate and filtered. The solvent was evaporated in a rotary evaporator to get the oil (2.8 g, 11.8 mmol) with 97% yield. ¹H NMR (CDCl₃) δ 0.01 (s, 6H), 0.85 (s, 9H), 3.58 (s, 2H), 4.55 (s, 2H), 6.56 (d, *J* = 8.6 Hz, 2H), 7.03 (d, *J* = 8.5 Hz, 2H).

***N*-(4-(Hydroxymethyl)phenyl)-2-phenylquinoline-4-carboxamide (4M).** To a 100 mL round-bottom flask equipped with a water condenser and a stir bar, potassium hydroxide (337 mg, 6 mmol) in ethanol (5 mL) was dissolved at 80 °C. Isatin (294 mg, 2 mmol) was added to the reaction mixture followed by dropwise addition of acetophenone (264 mg, 2.2 mmol). The mixture was refluxed at 80 °C for 3 days. Then the solvent was evaporated out using a rotary evaporator and the residue was dissolved in 50 mL of water. The aqueous phase was neutralized with dropwise addition of 1 N HCl to pH 6. The resulting solid was collected by vacuum filtration to get crude 2-phenylquinoline-4-carboxylic acid. The crude 2-phenylquinoline-4-carboxylic acid was used directly to get acyl chloride. To a 50 mL round-bottom flask equipped with a water condenser and a stir bar, the crude acid obtained above and 5 mL of neat thionyl chloride

were mixed. The mixture was refluxed at 80 °C for 2 h. After 2 h, excess thionyl chloride was evaporated using a stream of argon to get 2-phenylquinoline-4-carbonyl chloride. The resulting solid was dissolved in a 5:1 mixture of dichloromethane/triethylamine (5 mL), and 4-(*tert*-butylidimethylsilyloxy)methyl)aniline (473 mg, 2 mmol) in 1 mL of dichloromethane was added. The reaction mixture was stirred at room temperature for 2 h. Then the solvent was evaporated using a rotary evaporator and the crude product was purified by flash chromatography (30 g silica gel 60, 0.063–0.200 mm) using 25% ethyl acetate in hexanes to get 701 mg of *N*-(4-(*tert*-butylidimethylsilyloxy)methyl)phenyl)-2-phenylquinoline-4-carboxamide with 75% isolated overall yield in four steps. ¹H NMR (CDCl₃) δ 0.00 (s, 6H), 0.83 (s, 9H), 4.64 (s, 2H), 7.26 (d, *J* = 8.5 Hz, 2H), 7.31–7.42 (m, 4H), 7.58–7.64 (m, 3H), 7.77 (s, 1H), 7.94–8.06 (m, 5H); ESI-MS [*M* + *H*]⁺ = 369.4. *N*-(4-(*tert*-Butylidimethylsilyloxy)methyl)phenyl)-2-phenylquinoline-4-carboxamide (701 mg) was dissolved in 20 mL of tetrahydrofuran, and 2 mL of 1 M tetrabutylammonium fluoride solution in tetrahydrofuran was added. The reaction mixture was stirred, and the progress of the reaction was monitored by TLC. After the completion of reaction in 4 h, the solvent was evaporated and flash chromatography (30 g silica gel 60, 0.063–0.200 mm) was carried out to purify the product using hexane, dichloromethane, and methanol in 9:10:1 ratio. The product was crystallized in methanol/dichloromethane to get the title compound with 67% isolated yield. ¹H NMR (DMSO) δ 4.48 (d, *J* = 5.6 Hz, 2H), 5.18 (t, *J* = 5.6 Hz, 1H), 7.33 (d, *J* = 8.2 Hz, 2H), 7.52–7.61 (m, 3H), 7.68 (t, *J* = 8.2 Hz, 1H), 7.75 (d, *J* = 8.2 Hz, 2H), 7.84 (t, *J* = 8.2 Hz, 1H), 8.15 (d, *J* = 8.5 Hz, 2H), 8.33–8.37 (m, 3H), 10.79 (s, 1H); ¹³C NMR (DMSO) δ 65.58, 119.81, 122.76, 126.23, 128.11, 129.96, 130.36, 131.95, 132.65, 132.99, 133.34, 140.42, 141.14, 141.37, 146.09, 150.92, 158.84, 168.19, 225.16; ESI-MS [*M* + *H*]⁺ = 355.4.

■ ASSOCIATED CONTENT

● Supporting Information

Representative difference binding spectra for each series and synthesis and characterization data of substrates/metabolites. This material is available free of charge via the Internet at <http://pubs.acs.org>.

■ AUTHOR INFORMATION

Corresponding Author

*Phone: (509) 335-5983. Fax: (509) 335-8867. E-mail: jjp@wsu.edu.

■ ACKNOWLEDGMENTS

This work was supported by NIH Grant GM84546. Special thanks are extended to John T. Barr for valuable discussions during experiments and manuscript development.

■ ABBREVIATIONS USED

QCA, quinoline carboxamide; CYP, cytochrome P450; CYP3A4, cytochrome P450 3A4; V/K, in vitro metabolic intrinsic clearance; *K_M*, Michaelis–Menten constant; *k_{cat}*, turnover number

■ REFERENCES

- (1) Ortiz de Montellano, P. R. *Cytochrome P450: Structure, Mechanism, and Biochemistry*, 3rd ed.; Kluwer Academic/Plenum Publishers: New York, 2005.
- (2) Shimada, T.; Yamazaki, H.; Mimura, M.; Inui, Y.; Guengerich, F. P. Interindividual variations in human liver cytochrome P-450 enzymes involved in the oxidation of drugs, carcinogens and toxic chemicals: studies with liver microsomes of 30 Japanese and 30 Caucasians. *J. Pharmacol. Exp. Ther.* **1994**, *270*, 414–23.
- (3) Yamazaki, H.; Nakajima, M.; Nakamura, M.; Asahi, S.; Shimada, N.; Gillam, E. M.; Guengerich, F. P.; Shimada, T.; Yokoi, T.

Enhancement of cytochrome P-450 3A4 catalytic activities by cytochrome b(5) in bacterial membranes. *Drug Metab. Dispos.* **1999**, *27*, 999–1004.

(4) Evans, W. E.; Relling, M. V. Pharmacogenomics: translating functional genomics into rational therapeutics. *Science* **1999**, *286*, 487–491.

(5) Li, A. P.; Kaminski, D. L.; Rasmussen, A. Substrates of human hepatic cytochrome P450 3A4. *Toxicology* **1995**, *104*, 1–8.

(6) Dowers, T. S.; Rock, D. A.; Rock, D. A.; Perkins, B. N. S.; Jones, J. P. An analysis of the regioselectivity of aromatic hydroxylation and N-oxygenation by cytochrome P450 enzymes. *Drug Metab. Dispos.* **2004**, *32*, 328–32.

(7) Cooper, H. L.; Groves, J. T. Molecular probes of the mechanism of cytochrome P450. Oxygen traps a substrate radical intermediate. *Arch. Biochem. Biophys.* **2010**, *507*, 111–118.

(8) Das, A.; Sligar, S. G. Modulation of the cytochrome P450 reductase redox potential by the phospholipid bilayer. *Biochemistry* **2009**, *48*, 12104–12112.

(9) Jefcoate, C. R. Measurement of substrate and inhibitor binding to microsomal cytochrome P-450 by optical-difference spectroscopy. *Methods Enzymol.* **1978**, *52*.

(10) Schenkman, J. B. Studies on the nature of the type I and type II spectral changes in liver microsomes. *Biochemistry* **1970**, *9*, 2081–2091.

(11) Schenkman, J. B.; Remmer, H.; Estabrook, R. W. Spectral studies of drug interaction with hepatic microsomal cytochrome. *Mol. Pharmacol.* **1967**, *3*, 113–123.

(12) Ahlstrom, M. M.; Zamora, I. Characterization of type II ligands in CYP2C9 and CYP3A4. *J. Med. Chem.* **2008**, *51*, 1755–1763.

(13) Ballard, S. A.; Lodola, A.; Tarbit, M. H. A comparative study of 1-substituted imidazole and 1,2,4-triazole antifungal compounds as inhibitors of testosterone hydroxylations catalysed by mouse hepatic microsomal cytochromes P-450. *Biochem. Pharmacol.* **1988**, *37*, 4643–4651.

(14) Testa, B.; Jenner, P. Inhibitors of cytochrome P-450s and their mechanism of action. *Drug Metab. Rev.* **1981**, *12*, 1–117.

(15) Chiba, M.; Tang, C.; Neway, W. E.; Williams, T. M.; Desolms, S. J.; Dinsmore, C. J.; Wai, J. S.; Lin, J. H. P450 interaction with farnesyl-protein transferase inhibitors. Metabolic stability, inhibitory potency, and P450 binding spectra in human liver microsomes. *Biochem. Pharmacol.* **2001**, *62*, 773–776.

(16) Chiba, M.; Jin, L.; Neway, W.; Vacca, J. P.; Tata, J. R.; Chapman, K.; Lin, J. H. P450 interaction with HIV protease inhibitors: relationship between metabolic stability, inhibitory potency, and P450 binding spectra. *Drug Metab. Dispos.* **2001**, *29*, 1–3.

(17) Peng, C. C.; Pearson, J. T.; Rock, D. A.; Joswig-Jones, C. A.; Jones, J. P. The effects of type II binding on metabolic stability and binding affinity in cytochrome P450 CYP3A4. *Arch. Biochem. Biophys.* **2010**, *497*, 68–81.

(18) Pearson, J.; Dahal, U. P.; Rock, D.; Peng, C. C.; Schenk, J. O.; Joswig-Jones, C.; Jones, J. P. The kinetic mechanism for cytochrome P450 metabolism of type II binding compounds: evidence supporting direct reduction. *Arch. Biochem. Biophys.* **2011**, *511*, 69–79.

(19) Peng, C. C.; Rushmore, T.; Crouch, G. J.; Jones, J. P. Modeling and synthesis of novel tight-binding inhibitors of cytochrome P450 2C9. *Bioorg. Med. Chem.* **2008**, *16*, 4064–4074.

(20) Jones, J. P.; Joswig-Jones, C. A.; Hebner, M.; Chu, Y.; Koop, D. R. The effects of nitrogen-heme-iron coordination on substrate affinities for cytochrome P450 2E1. *Chem.-Biol. Interact.* **2011**, *193*, 50–56.

(21) Peng, C. C.; Cape, J. L.; Rushmore, T.; Crouch, G. J.; Jones, J. P. Cytochrome P450 2C9 type II binding studies on quinoline-4-carboxamide analogues. *J. Med. Chem.* **2008**, *51*, 8000–8011.

(22) Yano, J. K.; Denton, T. T.; Cerny, M. A.; Zhang, X.; Johnson, E. F.; Cashman, J. R. Synthetic inhibitors of cytochrome P-450 2A6: inhibitory activity, difference spectra, mechanism of inhibition, and protein cocrystallization. *J. Med. Chem.* **2006**, *49*, 6987–7001.

(23) Das, A.; Zhao, J.; Schatz, G. C.; Sligar, S. G.; Van Duyne, R. P. Screening of type I and II drug binding to human cytochrome P450-

3A4 in nanodiscs by localized surface plasmon resonance spectroscopy. *Anal. Chem.* **2009**, *81*, 3754–3759.

(24) Fleishaker, J. C.; Herman, B. D.; Carel, B. J.; Azie, N. E. Interaction between ketoconazole and almotriptan in healthy volunteers. *J. Clin. Pharmacol.* **2003**, *43*, 423–427.

(25) Vinh, T. K.; Ahmadi, M.; Delgado, P. O.; Perez, S. F.; Walters, H. M.; Smith, H. J.; Nicholls, P. J.; Simons, C. 1-[(Benzofuran-2-yl)phenylmethyl]-triazoles and -tetrazoles: potent competitive inhibitors of aromatase. *Bioorg. Med. Chem. Lett.* **1999**, *9*, 2105–2108.

(26) Korzekwa, K. R.; Jones, J. P.; Gillette, J. R. Theoretical studies on cytochrome P-450 mediated hydroxylation: a predictive model for hydrogen atom abstractions. *J. Am. Chem. Soc.* **1990**, *112*, 7042–7046.

(27) Korzekwa, K. R.; Jones, J. P. Predicting the cytochrome P450 mediated metabolism of xenobiotics. [Review]. *Pharmacogenetics* **1993**, *3*, 1–18.

(28) Jones, J. P.; Mysinger, M.; Korzekwa, K. R. Computational models for cytochrome P450: a predictive electronic model for aromatic oxidation and hydrogen atom abstraction. *Drug Metab. Dispos.* **2002**, *30*, 7–12.

(29) Olsen, L.; Rydberg, P.; Rod, T. H.; Ryde, U. Prediction of activation energies for hydrogen abstraction by cytochrome p450. *J. Med. Chem.* **2006**, *49*, 6489–6499.

(30) Porter, W. R.; Branchflower, R. V.; Trager, W. F. A kinetic method for the determination of multiple forms of microsomal cytochrome P-450. *Biochem. Pharmacol.* **1977**, *26*, 549–550.

(31) Roberts, A. G.; Campbell, A. P.; Atkins, W. M. The thermodynamic landscape of testosterone binding to cytochrome P 450 3A4: ligand binding and spin state equilibria. *Biochemistry* **2005**, *44*, 1353–1366.

(32) Omura, T.; Sato, R. The carbon monoxide binding pigment of liver microsomes. I. Evidence for its hemoprotein nature. *J. Biol. Chem.* **1964**, *239*, 2370–2378.

(33) McOmie, J. F. W.; Warrs, M. L.; West, D. E. Demethylation of aryl methyl ethers by boron tribromide. *Tetrahedron* **1968**, *24*, 2289–2292.

(34) Stenmark, H. G.; Brazzale, A.; Ma, Z. Biomimetic synthesis of macrolide/ketolide metabolites through a selective N-demethylation reaction. *J. Org. Chem.* **2000**, *65*, 3875–3876.

(35) Rosenau, T.; Hofinger, A.; Potthast, A.; Kosma, P. A general, selective, high-yield N-demethylation procedure for tertiary amines by solid reagents in a convenient column chromatography-like setup. *Org. Lett.* **2004**, *6*, 541–544.

(36) Acosta, K.; Cessac, J. W.; Rao, P. N.; Kim, H. K. Oxidative demethylation of 4-substituted N,N-dimethylanilines with iodine and calcium oxide in the presence of methanol. *Chem. Commun.* **1994**, 1985–1986.

(37) Dauben, H. J.; McCoy, L. L. N-Bromosuccinimide. III. Stereochemical course of benzylic bromination. *J. Am. Chem. Soc.* **1959**, *81*, 5404–5409.

(38) Barluenga, J.; Campos-Gomez, E.; Rodriguez, D.; Gonzalez-Bobes, F.; Gonzalez, J. M. New iodination reactions of saturated hydrocarbons. *Angew. Chem., Int. Ed.* **2005**, *44*, 5851–5854.

(39) Ghaffarzadeh, M.; Bolourtchiana, M.; Gholamhossenia, M.; Mohsenzadeha, F. Synthesis of arylaldehydes: Br₂/DMSO catalytic system for the chemoselective oxidation of methylarenes. *Appl. Catal. A* **2007**, *333*, 131–135.

(40) Nakanishi, M.; Bolm, C. Iron-catalyzed benzylic oxidation with aqueous *tert*-butyl hydroperoxide. *Adv. Synth. Catal.* **2007**, *349*, 861–864.

(41) Nicolaou, K. C.; Baran, P. S.; Zhong, Y. L. Selective oxidation at carbon adjacent to aromatic systems with IBX. *J. Am. Chem. Soc.* **2001**, *123*, 3183–3185.